Communications in Physics, Vol. 34, No. 3 (2024), pp. 227-236
DOI: https://doi.org/10.15625/0868-3166/20197

Mechanical and electric friction properties of Polymethyl methacrylate – Nitrocellulose blend polymer for triboelectric nanogenerators

Nguyen T. T. Duong[1,2], **Le T. T. Tam**[1,2], **Doan T. Tung**[1,†], **Nguyen T. Dung**[1], **Nguyen A. Duc**[3], **Ngo T. Dung**[1], **Phan N. Hong**[3], **Le T. Lu**[1] **and Phan N. Minh**[2,‡]

[1]*Institute for Tropical Technology, Vietnam Academy of Science and Technology, 18 Hoang Quoc Viet, Cau Giay, Hanoi, Vietnam*

[2]*Graduate University of Science and Technology, Vietnam Academy of Science and Technology, 18 Hoang Quoc Viet, Cau Giay, Hanoi, Vietnam*

[3]*Center for High Technology Development, Vietnam Academy of Science and Technology, 18 Hoang Quoc Viet, Cau Giay, Hanoi, Vietnam*

E-mail: [†]dtungtnt167@gmail.com; [‡]pnminh@vast.vn

Received 28 February 2024
Accepted for publication 31 July 2024
Published 21 August 2024

Abstract. *In this study, nitrocellulose - polymethyl methacrylate (NC/PMMA) blend film as a positive triboelectric material for triboelectric nanogenerator (TENG) with controlled flexibility was successfully synthesized by varying the PMMA content in the polymer blend. The combination of NC and PMMA reduced the limitations of the individual component materials with improved mechanical properties such as tensile strength, elastic modulus and elongation at breaking point. The TENG fabricated from NC/PMMA as a positive friction layer paired with fluorinated ethylene propylene (FEP) or polytetrafluoroethylene (PTFE) as a negative friction layer demonstrates a high peak to peak voltage output of 234 V at low frequency and with an actuation force of 10 N. The open circuit triboelectric voltage value maintains 91% durability after 26200 click-release cycles. This work provides a potential approach to simultaneously improve the electrical and mechanical properties of triboelectric materials, promoting the possibility of practical applications of TENG.*

Keywords: triboelectric nanogenerator (TENG); polymethyl methacrylate (PMMA); nitrocellulose (NC); polymer blend; energy conversion.

Classification numbers: 81.05.Lg; 41.20.Cv; 46.55.+d; 88.05.Gh.

1. Introduction

The rapid development of modern technology and the emergence of a series of smart devices in recent years have created an urgent need to develop independent, efficient, sustainable and highly flexible power sources. Triboelectric nanogenerators firstly invented in 2012 created a breakthrough in energy conversion and utilization technology and are considered potential candidates to replace conventional energy sources owing to theirs outstanding properties, including simple and flexible structural design, high output performance, low cost and abundant materials [1–3]. TENGs are mainly based on the Maxwell's displacement current, which can generate electrical energy by converting mechanical energy from the surrounding environment such as human motions, wind or water energies into electrical signals [4–7]. As a new mechanical energy harvesting system, TENGs have demonstrated great application potential in various fields of biomedical monitoring [8, 9], robot manufacturing, smart electronic devices, etc. [10, 11]. In addition, TENGs also demonstrate a superiority in manufacturing integrated power sources in self-powered active sensors and systems [12–14].

The working principle of TENG is based on the combination of the triboelectric effect and electrostatic induction. In TENG devices there must be at least two materials with different tribopolarities in the triboelectric series to generate electrical energy [15–17]. The pairs of contact materials used in TENGs commonly includes a positive triboelectric material and a negative triboelectric material, which are mounted on conductive substrates like Cu, Al, etc. The most commonly used positive materials for TENG are usually metal films of Cu, Al, Ag, and Au or polyamide (PA) [3]; while negative materials are usually polymers of polyvinylidene fluoride (PVDF), poly-dimethylsiloxane (PDMS) and polytetrafluoroethylene (PTFE) [18–20]. By combining suitable pairs of materials, the output performance of TENG is clearly enhanced.

Up to date, most of the materials used in TENGs are synthetic polymers due to their high mechanical and tribo-electric properties. However, the non-biodegradability and non-renewability limit their practical applications of TENGs [21, 22]. On the other hand, cellulose-based materials, especially nitrocellulose with biocompatibility and environmental friendliness, have attracted a great attention to fabricate components for TENGs in the recent years [23]. Nitrocellulose (NC) is an energetic polymer possessing unique properties such as high mechanical strength, excellent film-forming ability, etc., which has been used in a variety of fields, including medicine, coatings, electronics, biosensors, microelectronics and microfluidic devices [24–26]. Recently, NC-based materials have also been used to fabricate self-powered sensors [27]. Similar to NC, PMMA was used in TENGs as a positive friction material. The excellent triboelectric and high mechanical properties make PMMA an interesting material for TENGs [28]. However, sole PMMA is relatively brittle and inelastic. PMMA manufactured for contact-separation TENG will not have high durability. Therefore, combining NC with PMMA may be a solution to improve the lifespan of TENG devices, especially when operating in high humidity environments.

In this study, we combined NC and PMMA to create a NC/PMMA blend film for application as an electropositive friction electrode for TENGs. The influence of the NC/PMMA ratio on the mechanical and triboelectric properties of TENG has been studied to provide an optimal manufacturing plan in terms of mechanical strength while still maintaining good tribological properties. Finally, a contact-separate TENG structure consisting of NC/PMMA positive friction electrode

and fluorinated ethylene propylene (FEP) negative friction electrode achieves a high open-circuit peak-to-peak voltage value of 234 V.

2. Experiment

2.1. Materials

Commercial PMMA plastic pellets (ACRYPET-VH001) are obtained from Mitsubishi, Tokyo, Japan. WALSRODER™ Nitrocellulose FW 620 Isopropanol 35 % SD with high viscosity is ordered from DOW (USA). N,N-Dimethylformamide (DMF) is provided by Sigma Aldrich. Commercial polytetrafluoroethylene (PTFE) and fluorinated ethylene propylene (FEP) laminates with 0.05 mm thickness are purchased from Sigma Aldrich. Pure copper sheet (0.1 mm thickness) made in Vietnam. Two-component silver-graphene epoxy is produced by the Graphene Supermaket.

2.2. Fabrication of NC/PMMA polymer blend

The synthetic schematic illustration of NC/PMMA blend film is shown in Fig. 1. PMMA pellets and NC cottons were separately dissolved in DMF by stirring at 60℃ for 2 hours to obtain a homogeneous clear solution with a concentration of 0.3 %. Then, NC solution with various weight ratios of 0, 20, 50, 80 and 100 % was mixed into PMMA solution and continually stirred for 1 hour. The resulting solution was casted into a 10 x 10 cm^2 silica mold and dried in a vacuum oven at 60℃ for 24 hours to obtain NC/PMMA film material. The NC/PMMA film was peeled off from the silica mold after completely dried. The thickness of the NC/PMMA film was controlled $\sim$200 μm.

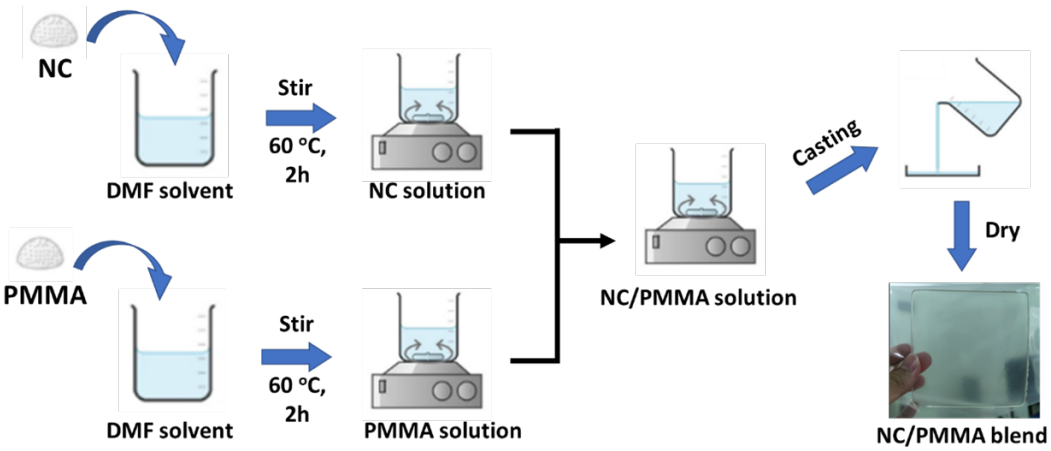

Fig. 1. Illustration of synthetic process of NC/PMMA blend.

2.3. Fabrication of nanogenerator

In this study, a TENG was fabricated by using a two-electrode vertical contact – separation mode. First, two Cu substrates were cut into a square of 10 cm × 10 cm. Next, the fabricated composite film was bonded to a Cu substrate as the positive triboelectric layer by using silver-graphene epoxy, while the FEP (or PTFE) layer was similarly bonded to another Cu substrate as

the negative triboelectric layer (Fig. 2). The obtained TENG devices were applied with an impact force of the same magnitude of 10 N with varying frequency. And the TENG test system is shown in Fig. 7b.

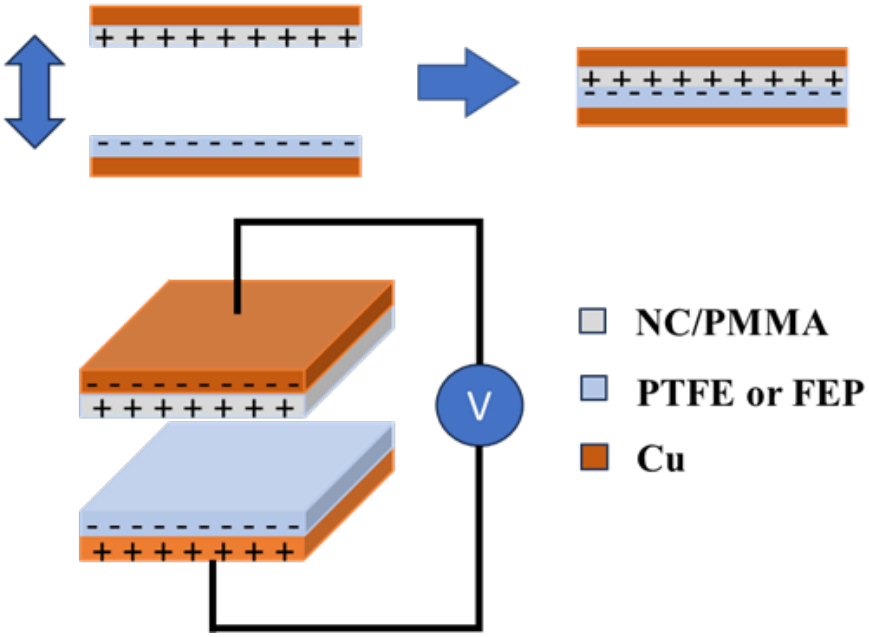

Fig. 2. TENG contact – separation structure of NC/PMMA with PTFE or FEP.

2.4. Characterization

FTIR spectra were recorded using a Nicolet 6700 FT-IR spectrometer in the wavenumber range of 4000–400 cm^{-1}.

The mechanical properties of the NC/PMMA blend including tensile strength, elongation at break and elastic modulus are determined on the ZWICK Z2.5 multifunction mechanical measuring device at room temperature with a crosshead speed of 50 mm/min according to the ASTM D638 standards.

Performance of the NC/PMMA-based TENGs was characterized based on open-circuit voltages by the Lecroy Wave Surfer 424 oscilloscope. The short-circuit currents (I_{sc}) of the device were amplified by a low-noise current preamplifier SR570.

3. Results and discussion

In Fig. 3a, the fabricated NC/PMMA TENG electrode with dimensions of 10 cm x 10 cm is relatively transparent. It can be seen that the membrane's surface made by casting method is high smoothness. This is more clearly in the SEM image (Fig. 3b). The surface of the material is completely homogeneous, dense and very flat.

Figure 3c shows the FTIR spectra of polymer blend at different NC/PMMA mass ratios. The FTIR spectrum of the pure NC film (100:0) indicates the absorption peaks at 3345 cm^{-1} and

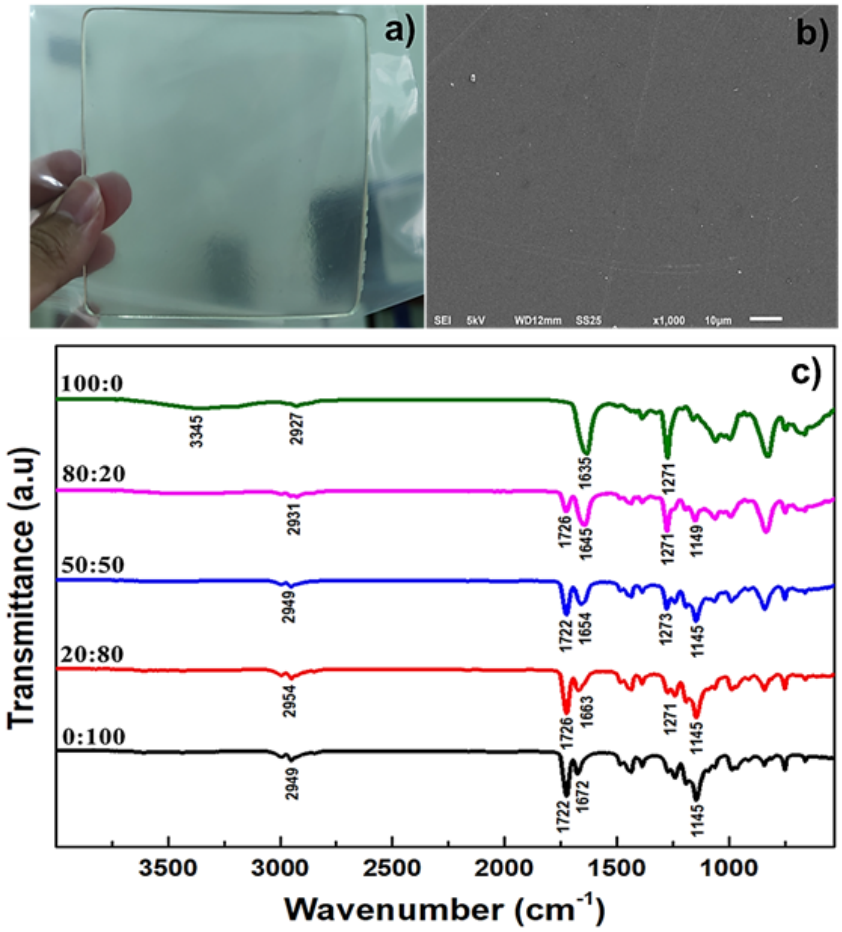

Fig. 3. a) NC/PMMA triboelectric film, b) SEM image of NC/PMMA film, c) FTIR spectra of NC/PMMA blend with various NC:PMMA mass ratio.

2927 cm^{-1}, which can be assigned to stretching vibration of O-H and C=O bonds, respectively. The most obvious absorption peaks at 1635 cm^{-1} and 1271 cm^{-1} are attributed to the asymmetric and symmetric stretching vibration of the -NO_2 group. The absorption peaks in the range of 1200 cm^{-1} to – 950 cm^{-1} are characterized for different vibrations of the C-O bond [26]. For sole PMMA (line e), the absorption peaks at 1722 cm^{-1}, 2949 cm^{-1}, 1672 cm^{-1} and 1145 cm^{-1} correspond to the vibration of the C=O, C-H, C=C and symmetric vibration of C-O-C bond, respectively [27].

For NC/PMMA blend others, FTIR spectra exhibit the appearance of characteristic absorption peaks of both NC and PMMA. However, it can be observed that the absorption peak of the -NO_2 group shifts towards larger wave numbers as the PMMA content gradually increases. Particularly, the absorption peak of -NO_2 group at 1635 cm^{-1} is shifted to 1645, 1654 and 1663 cm^{-1} corresponding to PMMA content of 20, 50 and 80 %, respectively. This is possible that the chemical interaction between the NO_2 group in NC and the C=C bond in PMMA occurs to form the NC/PMMA blend.

Fig. 4 shows tensile strength, elastic modulus and elongation at breaking point of NC/PMMA blend with different PMMA contents. From Fig. 4a, it can be seen that the tensile strength of pure NC film is higher than that of pure PMMA film. For NC/PMMA blend samples, the tensile strength gradually decreases when the PMMA content increases from 10 to 50 % wt, then increases slightly when the PMMA content reaches 80 % wt. The tensile strength values of the samples are 43.09, 31.36, 3.77 and 7.03 MPa, corresponding to PMMA content of 10, 20, 50, and 80 %. This trend is similar to the elastic modulus and elongation at break of NC/PMMA blend samples.

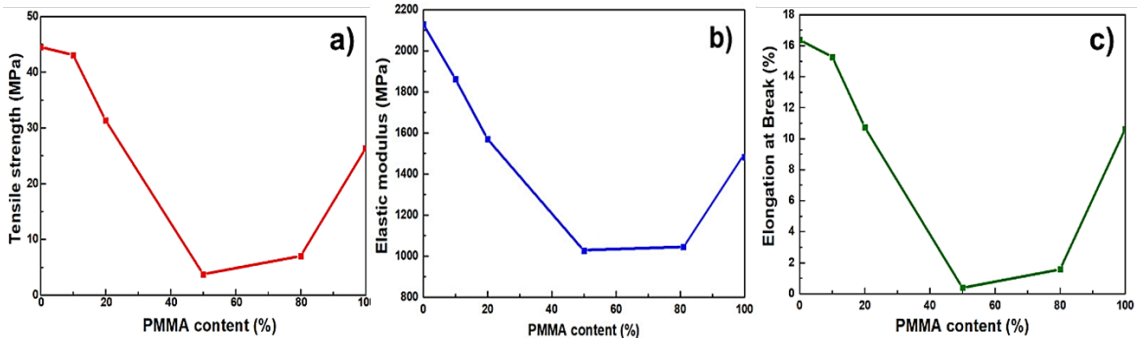

Fig. 4. a) Tensile strength, b) Elastic modulus curves and c) Elongation at breaking point of NC/PMMA blend with changing content of PMMA.

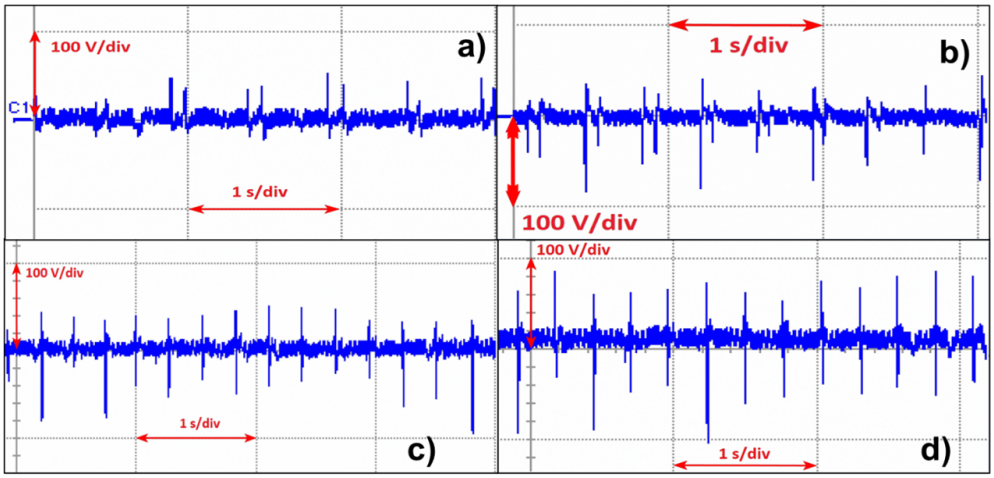

Fig. 5. OCV with the oscilloscope's 3-bit noise filter of NC/PMMA blend with different ratios: a) 100:0, b) 80:20, c) 20:80, d) 0:100.

To be able to choose the appropriate ratio between NC and PMMA in the triboelectric application, the electrode samples were also evaluated for open circuit voltage (OCV) with the 3-bit noise filter of the oscilloscope. Some comparison samples have the potential behavior after filtering with the PTFE negative electrode as shown in Fig. 5. At the same time, from the graph, the comparison table includes mechanical values along with electrical friction values listed in Table 1.

Table 1. Mechanical values and triboelectric potential of different NC/PMMA samples.

PMMA content (%)	Tensile strength (Mpa)	Elastic modulus (Mpa)	Elongation at Break (%)	V_{max}	V_{min}	V_{p-p}
0	44.52	2129.78	16.37	53.4	-42.2	95.6
10	43.09	1862.14	15.28	49.7	-51.7	101.4
20	31.36	1570.34	10.74	43.4	-84.4	127.8
50	3.77	1025.83	0.38	58.6	-86.9	145.5
80	7.03	1050.49	1.57	51.5	-95.1	146.6
100	26.36	1481.69	10.63	88.8	-103.0	191.8

The peak-to-peak triboelectric voltage of NC was significantly lower than that of PMMA (95.6 V vs. 191.8 V). The OCV increased with increasing PMMA content, indicating that PMMA had a high positive triboelectric charge. The 80:20 NC/PMMA blend retained good mechanical properties and better electromechanical conversion efficiency than pure NC.

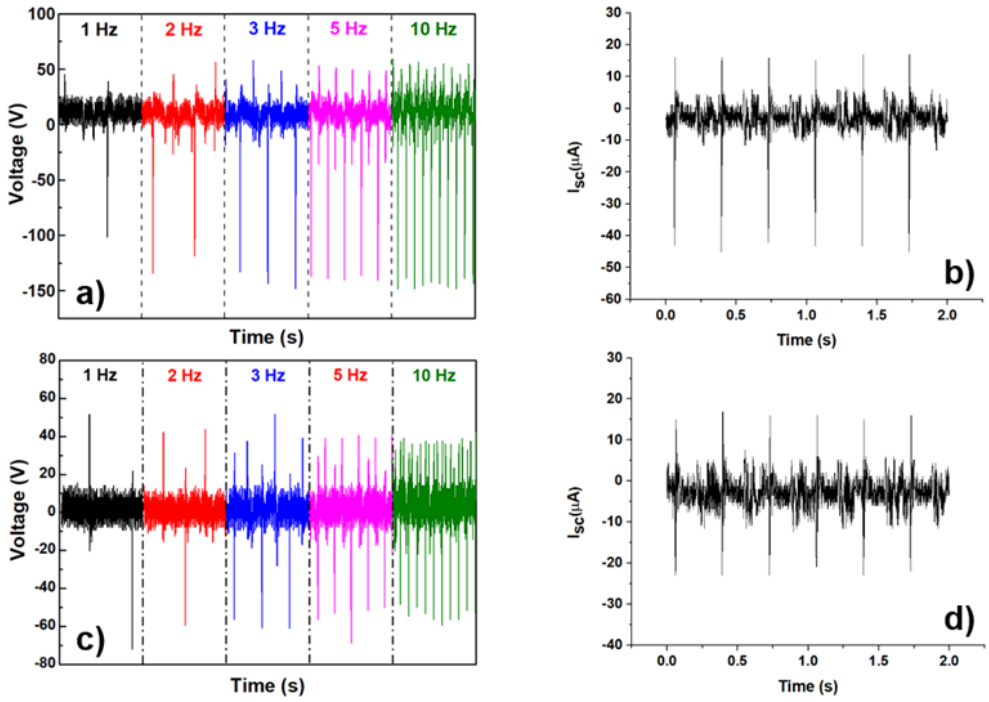

Fig. 6. OCV and I_{sc} of TENGs made from 80:20 NC/PMMA film and FEP (a,b) and PTFE (c,d).

To evaluate the output performance of 80:20 NC/PMMA-based TENG, the dependence of the output performance on the impact frequency was investigated. Fig. 6a and c show the relationship between the OCV without 3-bit noise filter and the impact frequency of 80:20 NC/PMMA-based TENG using FEP and PTFE as negative materials, respectively. It can be observed that the

output performance increases with increasing frequency from 1 to 10 Hz for NC/PMMA – FEP TENG while there is no significant change in the output voltage for NC/PMMA – PTFE TENG. This can be explained that the charge on the surface of the FEP sheet is not saturated while that on the PTFE sheet is saturated. The specific voltage values are given in Table 2. The FEP negative electrode also shows a better ability to generate electro-friction than PTFE. The peak-to-peak open circuit voltage of TENG with FEP reaches 234 V at 10 Hz interaction frequency, while it only reaches 112 V with PTFE. Similarly, for short-circuit current (Fig. 6 b,d), FEP also produced a larger current value than PTFE. However, the short-circuit current value achieved on both materials was only a few tens of μA, which is still quite modest.

Table 2. Maximum, minimum and peak-to-peak OCV values of TENG.

Frequency (Hz)	**NC/PMMA – FEP**			**NC/PMMA - PTFE**		
	$\mathbf{V_{max}}$	$\mathbf{V_{min}}$	$\mathbf{V_{p-p}}$	$\mathbf{V_{max}}$	$\mathbf{V_{min}}$	$\mathbf{V_{p-p}}$
1	56	-102	158	61	-73	134
2	58	-145	203	52	-67	119
3	58	-156	214	52	-64	116
5	59	-153	212	42	-69	111
10	78	-156	234	45	-67	112

Finally, the NC/PMMA TENG membrane was tested for durability after 26200 cycles compared to the FEP membrane. The TENG testing system is showed in Fig. 7b. The open-circuit voltage value was measured for the first 100 cycles and the last 100 cycles (Fig. 7a). The calculated results showed that the voltage value decreased by about 91% compared to the initial value. This shows that the NC/PMMA material has good mechanical strength and does not lose much in terms of electrical friction properties.

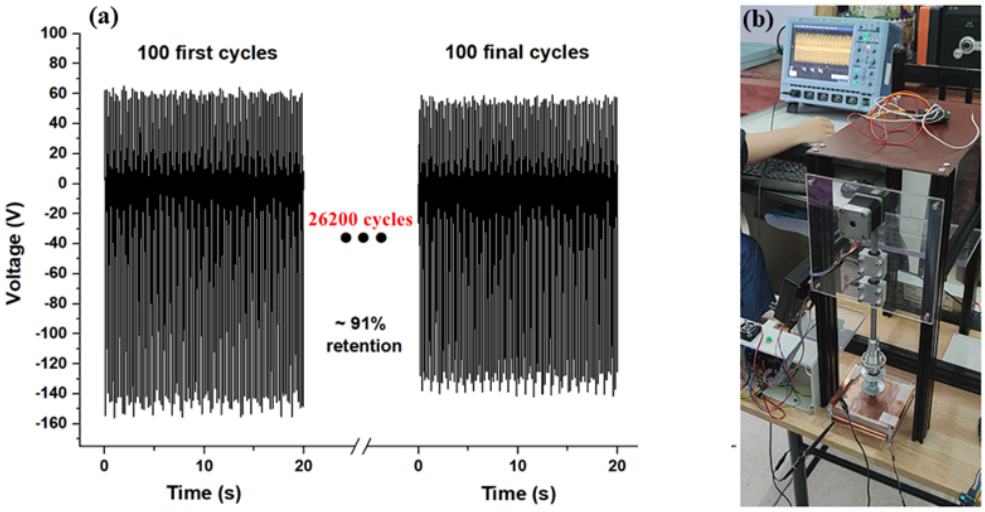

Fig. 7. a) Durability of the manufactured TENG fabricated from NC/PMMA and FEP; b) TENG testing system.

4. Conclusion

In summary, a NC/PMMA blend film based TENG with improved output performance and mechanical strength was proposed. By adding a suitable amount of PMMA to the NC matrix, the NC/PMMA blend film with controlled flexibility can be produced. The NC : PMMA ratio of 80 : 20 was chosen to give good mechanical properties while still achieving a high triboelectric effect. The TENG assembled by NC/PMMA film and FEP (or PTFE) as the positive and negative triboelectric layer respectively exhibits good triboelectric power generation effect. In which, the TENG device with FEP reaches a voltage that gradually increases with the impact frequency and has a maximum value of 234 V at a frequency of 10 Hz and an impact force of 10 N. A good triboelectric stability was demonstrated as the measured open circuit voltage remained at 91% after 26200 operating cycles. This may be feasible for triboelectric applications.

Acknowledgement

This word was funded from Vietnam Academy of Science and Technology under grant number DL0000.08/22-24.

Authors contributions

N.T.T. Duong, L.T.T. Tam and D.T. Tung fabricated the NC/PMMA electrodes. Nguyen T. Dung guided the process of sample drying and membrane separation. N.A. Duc mounted the electrode on the copper substrate. Ngo T. Dung measured membrane mechanical properties. P.N. Hong measured electro-tribological properties. L.T. Lu designed the experimental system and processed measurement data. P.N. Minh helped to supervise the project and improved the manuscript. All authors read and approved the final manuscript.

Conflict of interest

The authors declare that they have no competing financial interests.

References

[1] F.R. Fan, Z.Q. Tian, Z. Lin Wang, *Flexible triboelectric generator,* Nano Energy **1** (2012) 328.
[2] Z. L. Wang, J. Chen, L. Lin, *Progress in triboelectric nanogenerators as a new energy technology and self-powered sensors*, Energy Environ Sci. **8** (2015) 2250.
[3] C. Yao, X. Yin, Y. Yu, Z. Cai, X. Wang, *Chemically functionalized natural cellulose materials for effective triboelectric nanogenerator development*, Adv. Funct. Mater. **27** (2017) 1700794.
[4] Z.Y. Wu, B.B. Zhang, H.Y. Zou, Z.M. Lin, G.L. Liu, Z.L. Wang, *Multifunctional sensor based on translational-rotary triboelectric nanogenerator*, Adv. Energy Mater. **9** (2019) 1901124.
[5] K. Dong, X. Peng, Z.L. Wang, *Fiber/fabric-based piezoelectric and triboelectric nanogenerators for flexible/stretchable and wearable electronics and artificial intelligence*, Adv. Mater. **32** (2020) 1902549.
[6] C. Wang, Q.F. Shi, C.K. Lee, *Advanced implantable biomedical devices enabled by triboelectric nanogenerators*, Nanomaterials **12** (2022) 1366.
[7] Yu. Xie, Q. Ma, B. Yue, X. Chen, Y. Jin, H. Qi, Y. Hu, W. Yu, X. Dong, H. Jiang, *Triboelectric nanogenerator based on flexible Janus nanofiber membrane with simultaneous high charge generation and charge capturing abilities*, Chem. Eng. J. **452** (2023) 139393.
[8] J. Yang, J. Chen, Y. Su, Q. Jing, Z. Li, F. Yi, X. Wen, Z. Wang, Z. L. Wang, Eardrum-*Inspired active sensors for self-powered cardiovascular system characterization and throat-attached anti-interference voice recognition*, Adv. Mater. **27** (2015) 1316–1326.

[9] Z. Lin, J. Chen, X. Li, Z. Zhou, K. Meng, W. Wei, J. Yang, Z, L, Wang, *Triboelectric nanogenerator enabled body sensor network for self-powered human heart-rate monitoring*, ACS Nano **11** (2017) 8830.
[10] G. Schwartz, B.C.K. Tee, J. Mei, A. L. Appleton, D. H. Kim, H. Wang, Z. Bao, *Flexible polymer transistors with high pressure sensitivity for application in electronic skin and health monitoring*, Nat. Commun. **4** (2013) 1859.
[11] A. Leber, B. Cholst, J. Sandt, N. Vogel, M. Kolle, *Stretchable thermoplastic elastomer optical fibers for sensing of extreme deformations*, Adv. Funct. Mater. 2018 1802629.
[12] Z. Li, J. Chen, H. Guo, X. Fan, Z. Wen, M.-H. Yeh, C. Yu, X. Cao, *Triboelectrification-enabled self-powered detection and removal of heavy metal ions in wastewater*, Adv. Mater **28** (2016) 2983.
[13] Z. Li, J. Chen, J. Zhou, L. Zheng, K.C. Pradel, X. Fan, H. Guo, Z. Wen, M.-H. Yeh, C. Yu, Z. L. Wang, *High-efficiency ramie fiber degumming and self-powered degumming wastewater treatment using triboelectric nanogenerator*, Nano Energy **22** (2016) 548.
[14] Y. Xin, T. Du, T. Liu, P. Sun, M. Zhu, L. Zheng, H. Du, Y. Zou, M. Xu, *Triboelectric nanogenerator embedded cylindrical roller bearing for rotational energy harvesting and self-powered fault diagnosis*, Sensors and Actuators A: Physical **362** (2023) 114664.
[15] Y. Bai, H. Feng, Z. Li, *Theory and applications of high-voltage triboelectric nanogenerators*, Cell Rep. Phy. Sci. **3** (2022) 101108.
[16] L.S. McCarty, G.M. Whitesides, *Electrostatic charging due to separation of ions at interfaces: contact electrification of ionic electrets*, Angew. Chem. Int. Ed. 47 (2008) 2188–2207.
[17] H.T. Baytekin, A.Z. Patashinski, M. Branicki, B. Baytekin, S. Soh, B. A. Grzybowski, *The mosaic of surface charge in contact electrification*, Science **333** (2011) 308.
[18] C.H. Yao, A. Hernandez, Y.H. Yu, Z.Y. Cai, X.D. Wang, *Triboelectric nanogenerators and power-boards from cellulose nanofibrils and recycled materials*, Nano Energy **30** (2016) 103.
[19] Q. Zheng, L. Fang, H. Guo, K. Yang, Z. Cai, M.A.B. Meador, S. Gong, *Highly porous polymer aerogel film-based triboelectric nanogenerators*, Adv. Funct. Mater. **28** (2018) 1706365.
[20] K.Q. Xia, H.Z. Zhang, Z.Y. Zhu, Z.W. Xu, *Folding triboelectric nanogenerator on paper based on conductive ink and teflon tape*, Sensor and Actuator A: Phys. **272** (2018) 28.
[21] L. Liu, J. Pan, P. Chen, J. Zhang, X. Yu, X. Ding, B. Wang, X. Sun, H. Peng, *A triboelectric textile templated by a three-dimensionally penetrated fabric*, J. Mater. Chem. A **4** (2016) 6077.
[22] H. Li, S. Zhao, X. Du, J. Wang, R. Cao, Y. Xing, C. Li, *A compound yarn based wearable triboelectric nanogenerator for self-powered wearable electronics*, Adv. Mater. Technol. **3** (2018) 1800065.
[23] Y. Song, Z. Shi, G.-h. Hu, C. Xiong, A. Isogaid and Q. Yang, *Recent advances in cellulose-based piezoelectric and triboelectric nanogenerators for energy harvesting: a review*, J. Mater. Chem. A **9** (2021) 1910.
[24] L.R. Tang, W.X. Chen, B. Chen, R.X. Lv, X.Y. Zheng, C. Rong, B.L. Lu, B. Huang, *Sensitive and renewable quartz crystal microbalance humidity sensor based on nitrocellulose nanocrystals*, Sens. Actuators B-Chem. **327** (2020) 128944.
[25] W.Y. Wei, Y.P.Q. Yi, J. Song, X.G. Chen, J.H. Li, J.S. Li, *Tunable graphene/nitrocellulose temperature alarm sensors*, ACS Appl. Mater. Interfaces **14** (2022) 13790.
[26] R.H. Tang, M.Y. Xie, M. Li, L. Cao, S.S. Feng, Z.D. Li, F. Xu, *Nitrocellulose membrane for paper-based biosensor*, Appl. Mater. Today **26** (2022) 101305.
[27] T. Zheng, G. Li, L. Zhang, W. Sun, X. Pan, T. Chen, Y. Wang, Y. Zhou, J. Tian, Y. Yang, *A waterproof, breathable nitrocellulose-based triboelectric nanogenerator for human-machine interaction*, Nano Energy **114** (2023) 108649.
[28] T. Busolo, D. P. Ura, S. K. Kim, M. M. Marzec, A. Bernasik, U. Stachewicz, S. Kar-Narayan, *Surface potential tailoring of PMMA fibers by electrospinning for enhanced triboelectric performance*, Nano Energy **57** (2019) 500.